Chemistry & Biology, Vol. 8, 943–948, August, 2002, ©2002 Elsevier Science Ltd. All rights reserved. PII S1074-5521(02)00189-8

Cellular Import Mediated by Nuclear Localization Signal Peptide Sequences

Angela D. Ragin, Rashida A. Morgan, and Jean Chmielewski[1]
Department of Chemistry
Purdue University
West Lafayette, Indiana 47907

Summary

The cellular delivery of therapeutic agents and their localization within cells is currently a great challenge in medicinal chemistry. A few cationic peptides have shown a strong propensity to cross the cytoplasmic membrane and enter cells. Nuclear localization signal (NLS) sequences are a class of highly cationic peptides that may be exploited for cellular import of linked cargo. A series of NLS sequence peptides were investigated for entry into different cancer cell lines by flow cytometry and confocal microscopy. All NLS peptides demonstrated rapid accumulation within cells when added to the cellular media. Covalent adducts of proteins and oligonucleotides with NLS peptides were also effectively imported within cells. An understanding of the structural and mechanistic properties of these sequences will provide great potential for the rational design of efficient and selective peptidic delivery systems.

Introduction

The plasma membrane of cells presents a formidable barrier to the passage of a number of therapeutic agents and probes. The passive uptake of genes and polypeptides into cells is prohibitive due to size constraints, although smaller oligonucleotides and peptides are also too hydrophilic to adequately cross the hydrophobic bilayer [1]. The cell-impermeable nature of these biopolymers serves to underscore the need to develop efficient strategies for their cellular uptake. Numerous approaches have been employed to facilitate the import of DNA, for example, including viral vectors [2–3], cationic lipids [4], loligomers [5], and polylysine [6].

The seminal discovery that the HIV-1 Tat protein could travel across cell membranes in a receptor-independent fashion [7–8] resulted in studies to determine the minimal protein transduction domain of Tat [9–10]. Similar discoveries transpired with the Antennapedia (Antp) homeodomain protein [11–12]. This work has resulted in two peptide sequences, Tat (49–57) and Antp (43–58), with propensities to penetrate cell membranes and gain access to intracellular compartments. This cellular uptake also occurred while the peptides were attached to a wide range of cargoes, including proteins [13–14], oligonucleotides [14–15], imaging agents [16], iron oxide colloidal particles [17], and liposomes [18], and a Tat-β-galactosidase fusion protein was found to be delivered into all tissues in mice [19]. A few other peptide sequences have been identified with cell-translocating properties, including residues 267–300 of the viral protein VP22 [20]. Poly-arginine peptides [21] and cationic peptoids [22] have also been developed in this context. Although a number of mechanistic proposals have been put forth to explain the translocation of these hydrophilic peptides across the lipophilic cellular barrier, including endocytosis [23] and inverted micelle formation [14], the exact nature of this phenomenon has yet to be elucidated.

The importance of cationic peptides as delivery agents for therapeutics and probes, and the lack of a detailed mechanistic description, led us to search for other classes of peptides with transduction properties. One such class of cationic peptide sequences is that responsible for the transport of proteins into the nucleus from the cytoplasm. These sequences, known as nuclear localization signal sequences (NLS), are typically less than 12 residues in length, and, like the Tat and Antp peptides, are very rich in basic amino acids [24]. It seemed that these sequences could be exploited for uptake across the cytoplasmic membrane due to their cationic nature. These sequences would have the added advantage, however, of directing attached molecules to the nucleus, the site of action for numerous chemotherapeutic agents. To this end, we have evaluated NLS peptides derived from the transcription factors NF-κB, Oct-6, TFIIE-β, TCF1-α, SV40, HATF-3, and *C. elegans* SDC3 for cellular uptake and subcellular localization.

Results and Discussion

Fluorescently labeled nuclear localization signal sequences derived from transcription factors NF-κB, TFIIE-β, Oct-6, TCF1-α, SV40, HATF-3, and *C. elegans* SDC3 (Table 1) were synthesized by a solid phase approach. These sequences were chosen to evaluate the effect of varying the distribution of charged and uncharged residues within the peptides on cellular uptake. Each peptide was added to the media of MCF-7 (breast carcinoma) cells, and the resulting cells were evaluated by flow cytometry and confocal laser scanning microscopy. Flow cytometry studies revealed that all NLS peptides demonstrated rapid cellular accumulation when added to the media (Figure 1A).

Specific differences in the extent of uptake were observed, however, among the family of NLS sequences. Sequences containing the most cationic residues displayed the most effective cellular uptake profile with MCF-7 cells, which is consistent with previous experiments with homoarginine peptides [21]. Interestingly, Fl-TCF1-α, the sequence with the most cationic residues, was 2-fold less effective than Fl-Oct-6. This may be due to the Glu residue within Fl-TCF1-α, or the lower number of Arg versus Lys residues within its sequence. The NLS sequence with the poorest uptake, Fl-SDC3, contained only four cationic residues that were sepa-

[1]Correspondence: chml@purdue.edu

Table 1. Fluorescent Nuclear Localization Signal Sequences Used for Cellular Uptake Experiments

Fluorescent Peptides	Sequence
Fl-NF-κB	Fl-VQRKRQKLMP-NH_2
Fl-TFIIE-β	Fl-SKKKKTKV-NH_2
Fl-OCT-6	Fl-GRKRKKRT-NH_2
Fl-TCF1-α	Fl-GKKKKRKREKL-NH_2
Fl-SV40	Fl-PKKKRKV-NH_2
Fl-HATF3	Fl-ERKKRRRE-NH_2
Fl-*C.e.* SDC3	Fl-FKKFRKF-NH_2

rated and flanked by Phe residues. The presence of these residues within the NLS sequence may be responsible for the diminished cellular uptake.

To determine if cellular uptake of the NLS peptides could be extended beyond the MCF-7 cell line, and to obtain information regarding the scope of cell type specificity, four other cancerous cell types (KB, nasopharengeal; HT29, colon; MIAPACA2, pancreatic; PC3, prostate) were evaluated with a subset of NLS sequences. Cellular fluorescence was observed with all cell lines, demonstrating the ubiquitous nature of cellular uptake (Figure 1B). However, the amount of cellular fluorescence observed after exposure to the NLS peptides was distinctive for each of the cell types tested. This observation may provide a basis for future endeavors to integrate selectivity with NLS peptide uptake.

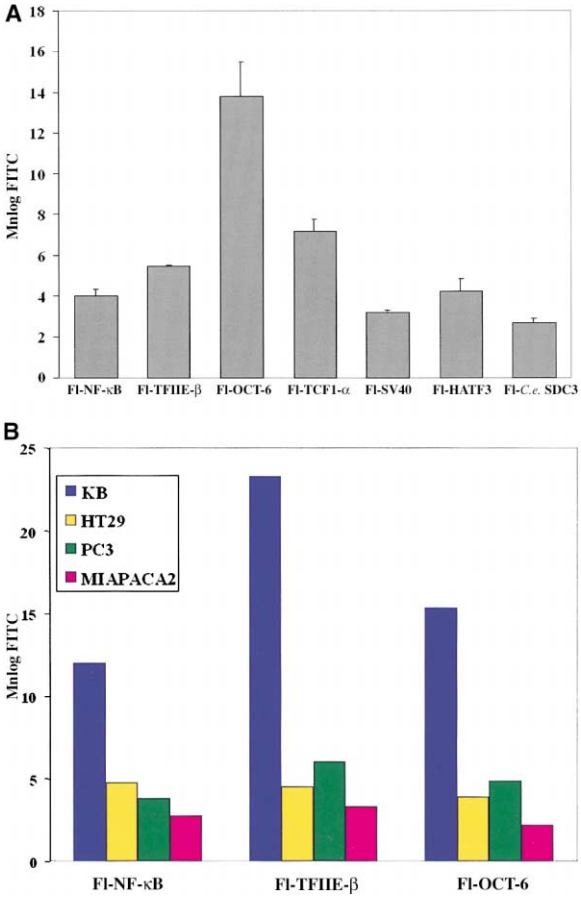

Figure 1. Cellular Uptake of Fluorescently Labeled NLS Sequences

(A) Uptake of fluorescently labeled NLS sequences (50 μM) with the MCF-7 (breast carcinoma) cell line after 4 hr as measured by flow cytometry.

(B) Uptake of the fluorescently labeled NLS sequences Fl-NF-κB, Fl-TFIIE-β, and Fl-Oct-6 (50 μM) with four other cancerous cell types—KB (nasopharengeal), HT29 (colon), MIAPACA2 (pancreatic), and PC3 (prostate)—after 4 hr as measured by flow cytometry.

The cellular location of a subset of NLS peptides, Fl-NF-κB, Fl-Oct-6, and Fl-TFIIE-β, was evaluated by confocal microscopy as these sequences demonstrated a range of values for cellular penetration. Confocal microscopy confirmed the presence of each peptide within the MCF-7 cell line. Interestingly, however, the subcellular localization of the tagged peptides was different for Fl-NF-κB (Figure 2) as compared to Fl-Oct-6 and Fl-TFIIE-β (Figures 3A and 3B, left). Fl-NF-κB was found distributed in both the cytosol and the nucleus, with greatest accumulation observed within nucleoli, whereas the other two sequences were located almost exclusively in the cytoplasm.

Mechanism Studies

In an effort to elucidate the mechanism of cellular penetration with NLS peptides, temperature and ATP-uncoupling experiments were carried out in MCF-7 cells. Receptor-mediated processes require ATP [25], and we found that the ATP uncouplers sodium azide [26] and 2,4-dinitrophenol [27] had no affect on cellular uptake with the NLS peptides. These data are in agreement with results obtained with Tat-linked liposomes [18], but are in disagreement with poly-arginine peptide experiments [21] in which a significant loss in cellular uptake was found as a function of added sodium azide. The data obtained with the NLS peptides indicate a process that is energy-independent, and therefore rule out a receptor-mediated transport pathway.

In general, decreases in temperature have had little effect on cellular uptake with cationic peptides. The uptake of the full length Tat protein, however, was almost completely inhibited at 4°C, leading the authors to conclude that uptake occurred via endocytosis [28]. Similar variations in temperature dependence were observed with the NLS sequences studied. Cellular uptake of the NLS sequences NF-κB, TFIIE-β, and HATF-3 was drastically reduced at 4°C, whereas, Oct-6, TCF1-α, SV40, and *C.e.* SDC3 showed little or no change. From both sets of experiments, we conclude that the NLS sequences of Oct-6, TCF1-α, SV40, and *C.e.* SDC3 enter cells by an energy independent, non-receptor-mediated process. However, it is more difficult to account mechanistically for the experimental data obtained with the NLS sequences NF-κB, TFIIE-β, and HATF-3. Membrane permeability is known to be decreased at reduced temperatures [29]. The effect of low temperature with these sequences on lowering uptake may point to a more direct means of lipid penetration that is still energy-independent. Neutralization of the charge of anionic membranes with cationic peptides has been shown to induce a lamellar to inverted hexagonal phase transition, resulting in membrane translocation through inverted micelle formation [30]. The NLS sequences described may utilize a similar mechanism for cellular uptake.

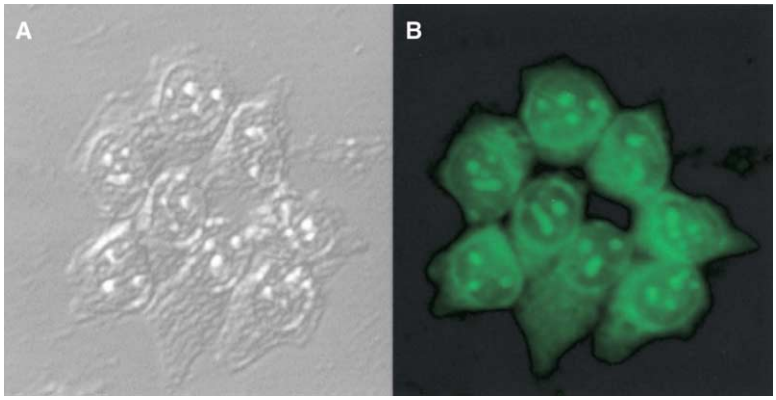

Figure 2. Confocal Microscopy of Fl-NF-κB-Treated MCF-7 Cells

Confocal microscopy of Fl-NF-κB (50 μM) treated MCF-7 cells after 4 hr. Transmitted light image (A) and fluorescence image (B) of Fl-NF-κB treated cells show nuclear localization.

Both Fl-TFIIE-β and Fl-Oct-6 were found by confocal microscopy to accumulate in the cytosol and appeared to be localized in endosomal compartments. Therefore, we carried out dual labeling experiments with a LysoTracker probe (Molecular Probes) to identify these structures. Following incubation of MCF-7 cells with the NLS peptides, labeling of acidic subcellular organelles was carried out by incubating the cells with 50 nM of the LysoTracker Red dye. The superimposed images (Figure 3, right) of cells containing the fluorescein-labeled NLS sequences (Figure 3, left) and LysoTracker dye (Figure 3, center) demonstrate that Fl-TFIIE-β and Fl-Oct-6 are entrapped within acidic compartments, such as endosomes or lysosomes, in the cytosol (Figures 2 and 3). Since the TFIIE-β and Oct-6 NLS peptides are highly cationic, they may tightly associate with negatively charged membrane lipids, precluding their release into the cytoplasm and subsequent routing to the nucleus. It is interesting to note that the NF-κB NLS sequence is able to escape from, or is never within, a similar endosomal compartment, a fact that perhaps points to a unique mode of cellular uptake for NF-κB.

Cellular Uptake of Covalently Coupled Cargoes

We exploited the membrane-translocating property of the NLS of NF-κB to deliver covalently linked cargoes across the plasma membrane of MCF-7 cells. A fluorescein-labeled, 10-mer oligonucleotide (5′-GCCTCTAGCT-3) derived from the Kras oncogene was covalently linked to the NLS of NF-κB via a disulfide linkage. Without the

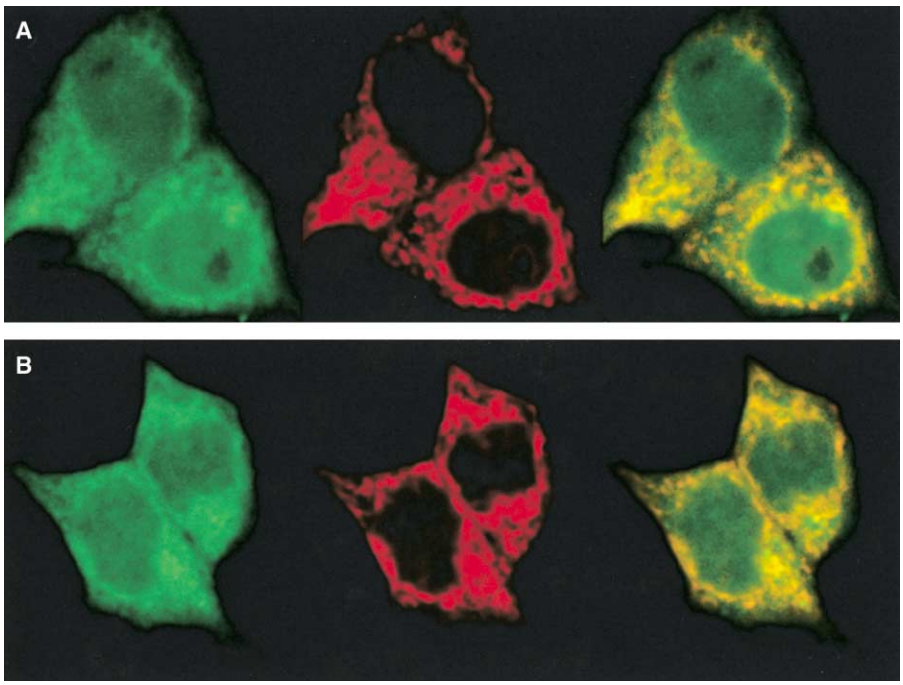

Figure 3. Dual Staining Experiments with Fluorescently Labeled NLS Sequences and MCF-7 Cells

Dual staining experiments were carried out using Fl-TFIIE-β (A) and Fl-Oct-6 (B) (50 μM) and the Lysotracker Red dye (50 nM) to stain acidic compartments within MCF-7 cells. Fluorescence images of MCF-7 cells visualized at 488 nm for fluorescein (left), at 568 nm for Lysotracker red (center), and overlay spectra from both (right) reveal that Fl-TFIIE-β and Fl-Oct-6 are localized within acidic compartments within the cytosol (yellow).

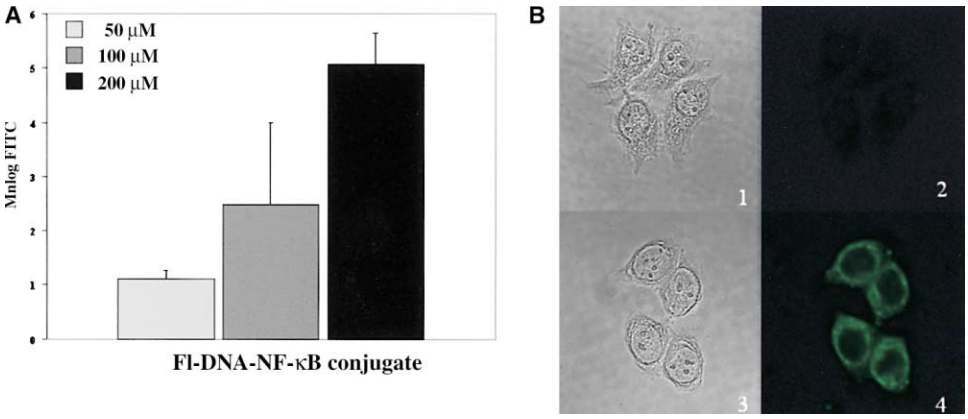

Figure 4. Cellular Uptake of the Fl-DNA-NF-κB Conjugate with MCF-7 Cells

(A) Cellular uptake as a function of concentration of the Fl-DNA-NF-κB conjugate with MCF-7 cells.

(B) Cellular localization was determined by confocal microscopy: (1) transmitted light image and (2) fluorescence image for cells treated with Fl-DNA (50 μM) for 4 hr; (3) transmitted light image and (4) fluorescence image for cells treated with Fl-DNA-NF-κB (50 μM) for 4 hr.

attached NLS sequence, the oligonucleotide displayed no propensity to enter MCF-7 cells (Figure 4B), whereas cellular uptake of the Fl-DNA-NF-κB conjugate was observed and found to increase with increasing concentration of the conjugate as shown by flow cytometry analysis (Figure 4A). Confocal microscopy images confirmed the presence of the oligonucleotide within the cells, and revealed that the conjugate had accumulated in the cytoplasm (Figure 4B).

The NF-κB sequence was also evaluated for transduction of the protein lysozyme. A Fl-lysozyme-NF-κB conjugate was prepared by first labeling lysozyme with NHS-fluorescein and activation of Fl-lysozyme with maleimide using Sulfo-SMCC (Sulfosuccinimidyl 4-[N-maleimidomethyl] cyclohexane-1-carboxylate; Pierce, Rockford, IL). This was followed by reaction of the resulting maleimide-activated Fl-lysozyme with an NF-κB sequence containing an N-terminal cysteine. Cellular uptake of the Fl-lysozyme-NF-κB conjugate (10 μM) was evaluated by flow cytometry and confocal microscopy in MCF-7 cells. Flow cytometry analysis revealed a 25-fold increase in cellular uptake of lysozyme when conjugated to the NF-κB NLS sequence (Figure 5A). Confocal microscopy revealed a highly punctate fluorescence pattern in the cytoplasm, a feature that is generally characteristic of endocytotic uptake (Figure 5B). A conjugate was also made between the NF-κB sequence and the protein β-galactosidase using the above method. A distinct increase in β-galactosidase activity was observed in MCF-7 cells that were treated with the β-galactosidase-NF-κB conjugate as compared to cells treated with β-galactosidase alone (Figure 6). These data confirm that biologically active proteins may be delivered to cells using this method.

Significance

The plasma membrane of living cells is lipophilic and the transport of large and charged molecules is restricted. The transmembrane transport of a number of pharmacologically relevant agents, such as proteins and oligonucleotides, is therefore limited. A small

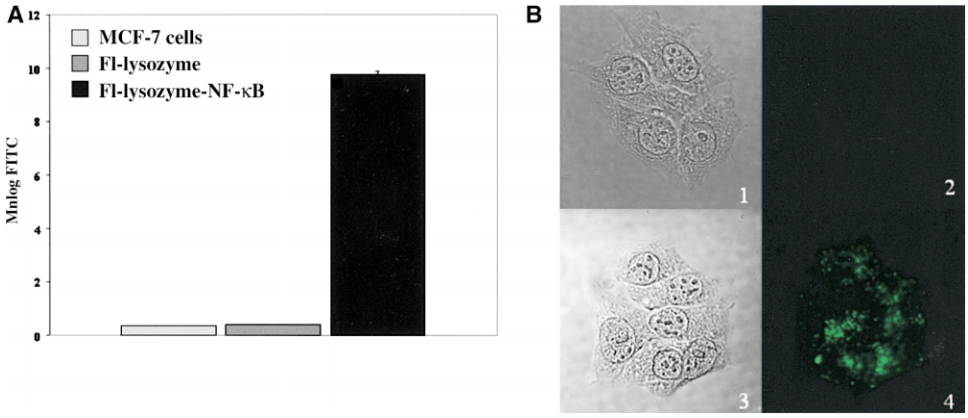

Figure 5. Cellular Uptake of Fl-Lysozyme-NF-κB Conjugate with MCF-7 Cells

(A) Cellular uptake of Fl-lysozyme with or without conjugation to NF-κB (10 μM) in MCF-7 cells after 4 hr.

(B) Cellular localization was determined by confocal microscopy: (1) transmitted light image and (2) fluorescence image for cells treated with Fl-lysozyme (10 μM) for 4 hr; (3) transmitted light image and (4) fluorescence image for cells treated with Fl-lysozyme-NF-κB (10 μM) for 4 hr.

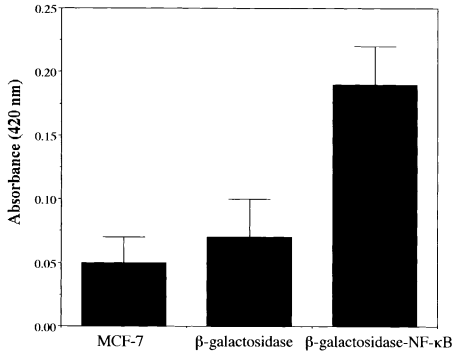

Figure 6. Quantitation of β-Galactosidase Activity in MCF-7 Cells

Quantitation of β-galactosidase activity in MCF-7 cells treated with β-galactosidase or β-galactosidase-NF-κB conjugate (50 μM each) for 4 hr. The chromogenic substrate o-nitrophenyl-β-D-galactopyranoside (ONPG) was used for determination of β-galactosidase activity (Sigma). The data are an average of three experiments.

class of cationic peptides have been identified with cellular transduction capabilities while attached to cargo such as DNA and proteins, and the current study sought to expand the repertoire of cationic peptides available for cellular import. Seven new peptide sequences with a range of cellular uptake propensities were identified in this work. Interestingly, the mechanism of uptake may be different among different classes of NLS cationic peptides, with some sequences accumulating in subcellular, acidic compartments, and others localizing in the nucleus. The NLS sequences assayed were found to target a wide range of cancerous cell types, providing a basis for future efforts to develop selective peptidic delivery systems. Additionally, the NLS of NF-κB successfully delivered covalent adducts of proteins and oligonucleotides to MCF-7 cells, thereby highlighting the promise of NLS sequences for novel, noninvasive delivery of agents of therapeutic value.

Experimental Procedures

Peptide Synthesis

All peptides were synthesized by a solid phase procedure on the Rink resin (Bachem). Fmoc was used as the semipermanent amine protecting group, and amino acid side chains were protected with tert-butyl-based functionality. Fluorescent analogs were synthesized by coupling NHS-fluorescein (Pierce) to the N terminus of the peptides while still attached to the resin. The crude peptides were purified to homogeneity by reverse phase HPLC (Waters Delta-Pak C8), and characterized by MALDI mass spectrometry and amino acid analysis.

Cell Culture

All cell lines were grown as adherent monolayers in a humidified 5% CO_2 atmosphere at 37°C. The cell lines were grown in the following culture media: MCF-7, RPMI (Roswell Park Memorial Institute); HT29, McCoy's 5A; PC3, Nutrient F12; KB and MIAPACA2, DMEM (Dulbecco's Modified Eagle's Medium). All media was supplemented with PS (100 units/ml penicillin and 0.1 mg/ml streptomycin) and 10% FCSHI (fetal calf serum heat activated). Nutrient F12 culture media was supplemented with 7% FCSHI.

Measuring Cellular Uptake

The cells were seeded into 24-well plates and grown in a humidified 5% CO_2 atmosphere at 37°C. The cells were incubated in the presence of the fluorescently labeled peptides at a concentration of 50 μM. Following incubation, the cells were washed with phosphate-deficient (Ca^{+2} and Mg^{+2} deficient buffer). The cells were gently dislodged from the wells with cell dissociation solution and resuspended in 200 μl of the appropriate culture media and 100 μl of PBS (pH 7.4). For each experiment, a control of cells that were not incubated with fluorescent peptide was also analyzed. Mean values of LogFITC fluorescence were measured on a Coulter Epics XL-MCL Flow Cytometer using an air-cooled laser for excitation of fluorescein at 488 nm.

ATP Uncoupling Experiments

ATP uncouplers, sodium azide (2 mM), and 2,4-dinitrophenol (2 mM) were added to MCF-7 cells seeded in 24-well plates and preincubated for 1 hr at 37°C prior to the addition of the fluorescently labeled peptides (50 μM). For each experiment, a control of cells that were incubated with sodium azide or 2,4-dinitrophenol was also analyzed. The samples were measured for cellular uptake as described above.

Temperature-Dependent Studies

Fluorescently labeled peptides (50 μM) were added to cells seeded in 24-well plates and incubated at either 4°C or 37°C. For each experiment, a control of cells that were not incubated with fluorescent peptides was also analyzed at 4° and 37°C, respectively. The samples were measured for cellular uptake as described above.

Confocal Microscopy

MCF-7 cells were seeded into LabTek chamber slide dishes in RPMI culture media supplemented with 10% FCSHI and PS. The cells were incubated in the presence of the fluorescently labeled NLS peptides at a concentration of 50 μM before confocal analysis. After incubation, the cells were washed with Ca^{+2} and Mg^{+2} deficient buffer, and the cells were fixed in a 100 μl of cold methanol. Fluorescent images were recorded on a Biorad Confocal Laser Scanning microscope. Images were recorded at slow speed using a 60× oil objective and a 488 nm laser for excitation of FITC.

LysoTracker Experiments

MCF-7 cells were seeded into LabTek chamber slide dishes in RPMI culture media supplemented with 10% FCSHI and PS. The cells were incubated in the presence of the fluorescently labeled NLS peptides at a concentration of 50 μM. After 4 hr, the LysoTracker probe (50 nM) was added and the cells were reincubated for an additional hour. The cells were washed with PBS (pH 7.4), fixed in neutral buffered formalin, and analyzed by confocal microscopy. Images were recorded at slow speed using a 60× oil objective and a 568 nm laser line for excitation of LysoTracker.

Oligonucleotide Conjugate Synthesis

The 5′-fluorescein-labeled, 10mer oligonucleotide (5′-GCCTCTA GCT-3′) containing a 3′ disulfide was purchased from Oligos Etc. The 3′-disulfide was reduced with excess dithiotreitol for 20 hr at 37°C in a pH 8.0 phosphate buffer. The resulting free thiol was treated with 2 equivalents of NLS-NF-κB containing an N-terminal cysteine activated with 2-dithiopyridine. The reaction was monitored by UV at 343 nm for maximum release of thiopyridone, and after 13 hr, the reaction mixture was purified by Sephadex G50 size exclusion chromatography.

Lysozyme Conjugate Synthesis

Lysozyme was labeled with NHS-fluorescein in a pH 8.5 sodium carbonate buffer for 2 hr, and purified by Sephadex G50 size exclusion chromatography. Mass spectrometry indicated the modification with four fluorescein molecules. The fluorescently labeled lysozyme (Fl-lysozyme) was activated with maleimide using 10 equivalents of sulfosuccinimidyl 4-(N-maleimidomethyl) cyclohexane-1-carboxylate (Sulfo-SMCC, Pierce, Rockford, IL) in a pH 8.5 sodium carbonate buffer for 2 hr. The maleimide activated Fl-lysozyme conjugate was reacted with 10 equivalents of NLS-NF-κB containing an N-terminal cysteine in PBS buffer for 2 hr. The conjugate was purified by Sephadex G50 size exclusion chromatography, and mass spectrometry indicated the attachment of two NLS-NF-κB peptides.

Acknowledgments

We are grateful to Dr. Michelle Brickner for initiating work in this area, and Professor Paul Robinson for confocal microscopy and flow cytometry training and instrument time. A.D.R. and R.A.M. were supported by predoctoral fellowships from NIH.

Received: December 13, 2001
Revised: July 2, 2002
Accepted: July 25, 2002

References

1. Dokka, S., and Rojanasakul, Y. (2000). Novel non-endocytotic delivery of antisense oligonucleotides. Adv. Drug Deliv. Rev. *44*, 35–49.
2. Hu, W.-S., and Pathak, V.K. (2000). Design of retroviral vectors and helper cells for gene therapy. Pharmacol. Rev. *52*, 493–511.
3. Smith, A.E. (1995). Viral vectors in gene therapy. Annu. Rev. Microbiol. *49*, 807–838.
4. Chesnoy, S., and Huang, L. (2000). Structure and function of lipid-DNA complexes for gene delivery. Annu. Rev. Biophys. Biomol. Struct. *29*, 27–47.
5. Devender, S., Reza, K., Kawamura, K., LaCasse, E.C., and Gariepy, J. (1998). Penetration and intracellular routing of nucleus-directed peptide-based shuttles (loligomers) in eukaryotic cells. Biochemistry *37*, 5798–5809.
6. Leonetti, J.P., Degols, G., and Lebleu, B. (1990). Biological activity of oligonucleotide-poly-(L-lysine) conjugates. Bioconjug. Chem. *1*, 149–153.
7. Frankel, A.D., and Pabo, C.O. (1988). Cellular uptake of the Tat protein from human immunodeficiency virus. Cell *55*, 1189–1193.
8. Green, M., and Loewenstein, P.M. (1988). Autonomoius functional domains of chemically synthesized HIV Tat trans-activator protein. Cell *55*, 1179–1188.
9. Fawell, S., Seery, J., Daikh, Y., Moore, C., Chen, L.L., Pepinsky, B., and Barsoum, J. (1994). Tat-mediated delivery of heterologous proteins into cells. Proc. Natl. Acad. Sci. USA *91*, 664–668.
10. Vives, E., Brodin, P., and Lebleu, B. (1997). A truncated HIV-1 Tat protein basic domain rapidly translocates through the plasma membrane and accumulates in the cell nucleus. J. Biol. Chem. *272*, 16010–16017.
11. Derossi, D., Joliot, A.H., Chassaing, G., and Prochiantz, A. (1994). The third helix of the Antennapedia homeodomain translocates through biological membranes. J. Bio. Chem. *269*, 10444–10450.
12. Derossi, D., Calvert, S., Trembleau, A., Brunissen, A., Chassaing, G., and Prochiantz, A. (1996). Cell internalization of the third helix of the Antennapedia homeodomain is receptor-independent. J. Biol. Chem. *271*, 18188–18193.
13. Schwarze, S.R., Hruska, K.A., and Dowdy, S.F. (2000). Protein transduction: Unrestricted delivery into cells. Trends Cell Biol. *10*, 290–296.
14. Derossi, D., Chassaing, G., and Prochiantz, A. (1998). Trojan peptides: The Penetratin system for intracellular delivery. Trends Cell Biol. *8*, 84–87.
15. Eguchi, A., Akuta, T., Okuyama, H., Senda, T., Yokoi, H., Inokuchi, H., Fujita, S., Hayakawa, T., Takeda, K., Hasegawa, M., et al. (2001). Protein transduction domain of HIV-1 Tat protein promotes efficient delivery of DNA into mammalian cells. J. Biol. Chem. *276*, 26204–26210.
16. Polyakov, V., Sharma, V., Dahlheimer, J., Pica, C., Luker, G., and Piwnica-Worms, D. (2001). Novel Tat-peptide chelates for direct transduction of technetium-99m and rhenium into human cells for imaging and radiotherapy. Bioconjug. Chem. *11*, 762–771.
17. Lewin, M., Calesso, N., Tung, C.H., Tang, X.W., Cory, D., Scadden, D.T., and Weissleder, R. (2000). Tat peptide derivatized magnetic nanoparticles allow in vivo tracking and recovery of progenitor cells. Nat. Biotechnol. *18*, 410–414.
18. Torchilin, V., Rammohan, R., Weissig, V., and Levchenko, T. (2001). Tat peptide on the surface of liposomes affords their efficient intracellular delivery even at low temperature and in the prescence of metabolic inhibitors. Proc. Natl. Acad. Sci. USA *98*, 8786–8791.
19. Schwarze, S.R., Ho, A., Vocero-Akbani, A., and Dowdy, S.F. (1999). In vivo protein transduction of a biologically active protein into the mouse. Science *285*, 1569–1572.
20. Elliot, G., and O'Hare, P. (1997). Intracellular trafficking and protein delivery by a Herpesvirus structural protein. Cell *88*, 223–233.
21. Mitchell, D.J., Kim, D.T., Steinman, L.C., Fathman, C.G., and Rothbard, J.B. (2000). Polyarginine enters cells more efficiently than other polycationic homopolymers. J. Pept. Res. *55*, 318–325.
22. Wender, P.A., Mitchell, D.J., Pattabiraman, K., Pelkey, E.T., Steinman, L., and Rothbard, J.B. (2000). The design, synthesis and evaluation of molecules that enable or enhance cellular uptake. Peptoid Molecular Transporters. Proc. Natl. Acad. Sci. USA *97*, 13003–13008.
23. Lindgren, M., Hallbrink, M., Prochiantz, A., and Langel, U. (2000). Cell penetrating peptides. Trends Prot. Sci. *21*, 99–103.
24. Boulikas, T. (1994). Putative nuclear localization signals (NLS) in protein transcription factors. J. Cell. Biochem. *55*, 32–58.
25. Schmid, S., and Carter, L.L. (1990). ATP is required for receptor-mediated endocytosis in intact cells. J. Cell Biol. *111*, 2307–2315.
26. Sandvig, K., and Olsnes, S. (1982). Entry of toxic proteins abrin, modeccin, ricin, and diptheria toxin into cells. J. Biol. Chem. *257*, 7504–7513.
27. Skulachev, V. (1998). Uncoupling: New approaches to an old problem of bioenergetics. Biochim. Biophys. Acta *1363*, 100–124.
28. Mann, D.A., and Frankel, A.D. (1991). Endocytosis and targeting of exogenous HIV-1 Tat protein. EMBO J. *10*, 1733–1739.
29. Frezard, F., and Garnier-Suillerot, A. (1998). Permeability of lipid bilayer to Anthracycline derivatives. Role of the bilayer composition and of the temperature. Biochim. Biophys. Acta *1389*, 13–22.
30. Belrose, J.P., Convert, O., Derossi, D., Brunissen, A., Chassaing, G., and Prochiantz, A. (1996). Conformational and associative behaviors of the third helix of Antennapedia homeodomain in membrane-mimetic environment. Eur. J. Biochem. *242*, 372–386.